Lv et al. Critical Care (2025) 29:272
https://doi.org/10.1186/s13054-025-05514-4

Critical Care

RESEARCH Open Access

Respiratory effort monitoring: a novel, bedside, non-invasive, real-time method

Yinxia Lv[1†], Meiling Dong[1†], Haisong Song[2†], Jinglei Liu[2†], Zhiwen Huang[2], Zhong Ni[1], Zhen Wang[1], Xiaorong Jing[1], Xiaoyong Zhou[2], Yongfang Zhou[1*], Yan Kang[3,4*] and Bo Wang[3*]

Abstract

Background Mechanical ventilation is essential for treating respiratory failure. However, ventilator over-assistance can lead to ventilator-induced diaphragm dysfunction (VIDD), and insufficient assistance can necessitate excessive effort, which leads to high stress and damage diaphragm function. Current methods monitoring respiratory effort face clinical implementation challenges due to invasiveness and complexity. This study introduces and validates a novel non-invasive real-time respiratory muscle pressure (N-Pmus) monitoring method.

Methods (1) The bench study involved developing a non-invasive, real-time respiratory muscle pressure monitoring algorithm (N-Pmus) based on the equation of motion of the respiratory system and validated with efforts generated by the ASL simulator (ASL5000-Pmus) across 270 clinical scenarios. (2) A clinical validation was performed through a prospective observational study ($n=23$), comparing N-Pmus with the Pmus derived from simultaneously monitored esophageal pressure ($Pmus_{eso}$) to assess correlation and agreement. The association between N-Pmus and the established Pmus benchmarks was analyzed using linear mixed-effects models. Bias and agreement were evaluated through Bland–Altman analysis for repeated measures.

Results (1) The bench study demonstrated that N-Pmus correlated well with ASL5000-Pmus, with marginal R^2=0.993 and conditional R^2=0.997. The bias was −0.23 cmH_2O, with limits of agreement ranging from −1.51 to 1.04 cmH_2O. (2) The clinical validation revealed strong N-Pmus/$Pmus_{eso}$ agreement with marginal R^2=0.97 and conditional R^2=0.971. The bias was −0.2 cmH_2O, with limits of agreement ranging from −2.22 to 1.83 cmH_2O.

Clinical trial number Retrospectively registered with https://www.chictr.org.cn/. Registration number: ChiCTR2300076940, registered 24 October 2023.

Keywords Mechanical ventilation, Respiratory effort, Non-invasive monitoring, Respiratory muscle pressure (Pmus)

†Yinxia Lv, Meiling Dong, Haisong Song and Jinglei Liu contributed equally.

*Correspondence:
Yongfang Zhou
zyfmg@163.com
Yan Kang
kangyan@scu.edu.cn
Bo Wang
drwangbowch@163.com

[1]Department of Respiratory Care, West China Hospital of Sichuan University, Chengdu 610041, China
[2]Shenzhen Mindray Bio-Medical Electronics Co.,Ltd., Shenzhen 518057, China
[3]Department of Critical Care Medicine, West China Hospital of Sichuan University, Chengdu 610041, China
[4]Department of Critical Care Medicine, West China Tianfu Hospital, Sichuan University, 610218 Chengdu, China

Background

Mechanical ventilation stands as a critical intervention for patients grappling with respiratory failure, while its improper usage can potentially lead to ventilator associated injury [1–3]. During the process of mechanical ventilation, ventilator over-assistance may result in insufficient breathing effort, ultimately contributing to atrophy and weakness of the diaphragm. Conversely, insufficient assistance can necessitate excessive effort, which leads to high stress and damage diaphragm function. Vigorous effort can significantly elevate local lung stress and strain, potentially resulting in injurious transpulmonary pressure, pendelluft, and asynchrony with ventilator, thereby inciting or exacerbating patient self-inflicted lung injury (P-SILI) [4]. Furthermore, excessive breathing effort could incite eccentric contractions of diaphragm, which have been shown to cause sarcolemmal disruption and inflammation on a microscopic scale in animal models, so called load injury [5].

Ventilator-induced diaphragm dysfunction (VIDD) due to underuse or overuse of the diaphragm is frequently encountered in critically ill mechanical ventilated patients, which is associated with prolonged mechanical ventilation and poor prognostic outcomes [6]. Therefore, precise and reliable monitoring of respiratory effort is of paramount importance to maintain appropriate effort and prevent both VIDD and P-SILI. Currently, bedside routine methodologies for the direct assessing breathing effort include esophageal pressure (Pes) [7, 8], end-inspiratory airway occlusion pressure (PMI) [9], and end-expiratory airway occlusion pressure (Pocc) [10]. Additionally, diaphragm electromyography (EAdi) [11, 12], and diaphragm ultrasound [13] are employed for the indirect evaluation of breathing effort. These methodologies require manual oversight by medical professionals or respiratory therapists, and the use of diaphragm electromyography and esophageal pressure catheter insertion involve invasive procedures, which carry inherent risks in clinical application. Furthermore, the assessment of diaphragm ultrasound poses specific challenges in clinical execution [14, 15]. At present, a straightforward, non-invasive, and continual monitoring modality is lacking in clinical praxis to accurately gauge the strength of patients' spontaneous respiratory efforts.

This study developed an innovative noninvasive approach for real-time dynamic monitoring of spontaneous breathing effort (N-Pmus), achieved by modeling respiratory mechanics through mathematical optimization algorithms, thereby eliminating the need for catheter insertion. Subsequently, simulated scenarios and clinical trials were conducted to compare N-Pmus with the bedside routine Pmus measurement ($Pmus_{eso}$) to confirm their correlation and alignment. Furthermore, subgroup analyses encompassing a variety of conditions, ventilation modalities, and levels of respiratory effort were performed to further validate these findings.

Methods

Study design

The study comprised two distinct steps (Fig. 1). In Step One, termed the Bench study, a real-time algorithm for monitoring N-Pmus was developed and integrated into a ventilator platform (SV800, Mindray, Shenzhen, China). An experimental setup was established using the Active Servo Lung 5000 (ASL 5000, IngMar Medical, Pittsburgh, PA, USA) and the ventilator to validate its accuracy by comparing N-Pmus with ASL5000-Pmus. Step Two involved clinical validation through a single-center, prospective observational trial conducted in 2023 in the ICUs of West China Hospital, Sichuan University. N-Pmus was compared with simultaneously monitored $Pmus_{eso}$ to assess its clinical correlation and agreement. The study was approved by the Ethics Committee of West China Hospital, Sichuan University (Ethics Approval No. 2023 Approval (105)), and informed consent was obtained from all participants before enrollment. The study is registered under ChiCTR2300076940.

Bench study

The N-Pmus algorithm was developed based on the equation of motion of the respiratory system:

$$P_{aw}(t) = \dot{V}(t) * R_{rs} + \frac{V(t)}{C_{rs}} + P_{mus}(t) + P_0 \quad (1)$$

Here, $P_{aw}(t)$ (airway pressure), $\dot{V}(t)$ (flow), and $V(t)$ (volume, derived from flow integration) are time-dependent values measured by ventilator sensors. The unknowns include three constants: R_{rs} (respiratory system resistance), C_{rs} (respiratory system compliance), and P_0 (end-expiratory pressure), as well as the time-varying respiratory muscle pressure $P_{mus}(t)$. Directly solving for these variables is infeasible due to an underdetermined system (fewer equations than unknowns). To address this, the morphology of $P_{mus}(t)$ is modeled using a physiologically plausible polynomial function—specifically, a cubic function template that accounts for active expiration—and reduces the number of unknown variables. The detailed derivation is provided in the Additional file, with corresponding illustrations shown in Figure E1. This reformulates the system into an overdetermined framework (more equations than unknowns), solvable via iterative least-squares optimization [16].

The experiment utilized an ASL5000 simulator in conjunction with an SV800 ventilator to simulate three clinical scenarios: normal (compliance: 50 mL/cmH_2O; resistance: 10 cm H_2O/L/s), restrictive (compliance: 20, 30, 40 mL/cmH_2O; resistance: 13 cmH_2O/L/s), and

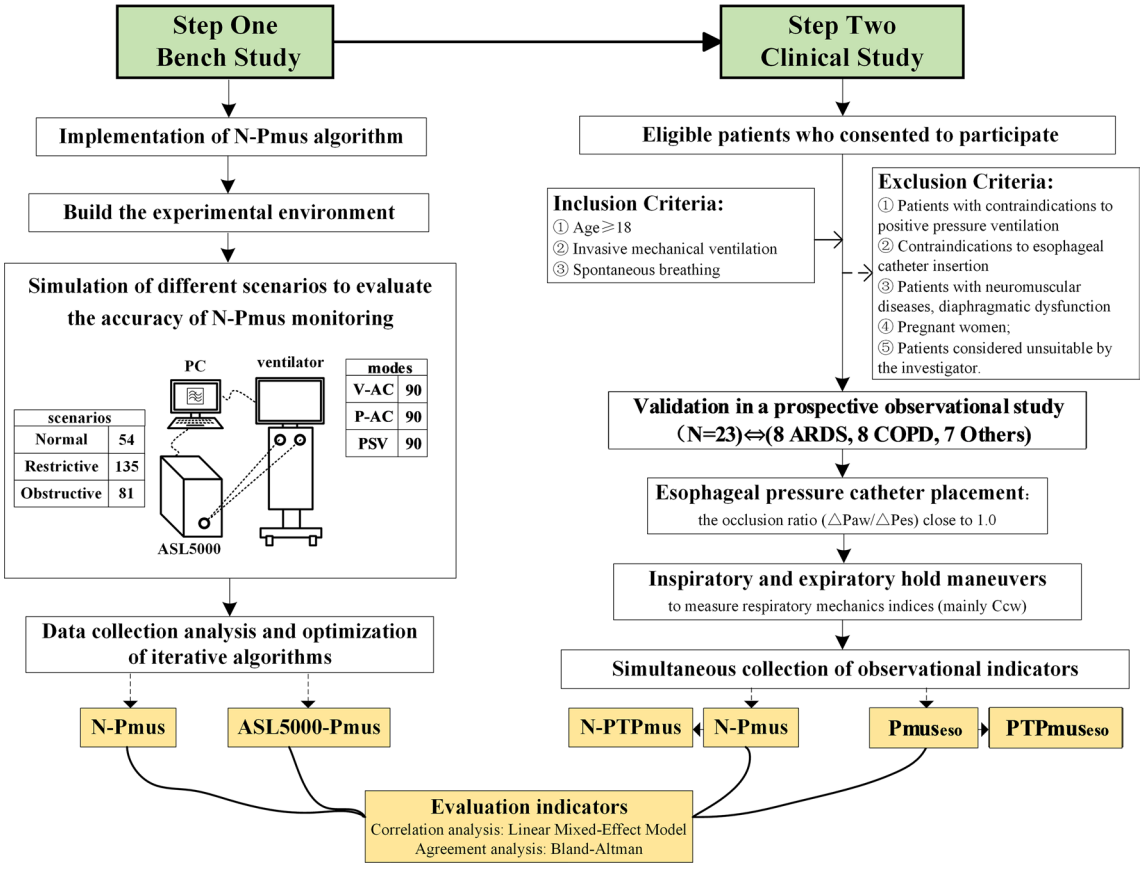

Fig. 1 Studies performed and flowchart

obstructive (compliance: 60 mL/cmH_2O; resistance: 15, 20, 25 cmH_2O/L/s), following established benchmarks [17, 18]. Spontaneous breathing was modeled using programmable sinusoidal patient muscle pressure (P_{mus}) waveforms (intensity: 3, 5, 6, 9, 10, 12, 15, 18, 20, 25, and 30 cmH_2O), with adjustable rise (10%, 20%) and release (10%, 20%, 30%) phases to replicate varied effort profiles (see Additional file: Table E1).

Clinical study

The study flowchart, including the inclusion and exclusion criteria, is summarized in Fig. 1. Comprehensive procedural details are documented in the Additional file.

Study population

Three groups of patients were enrolled to this study: (1) acute respiratory distress syndrome (ARDS) per Berlin definition [19], (2) chronic obstructive pulmonary disease (COPD) per GOLD guidelines [20], and (3) non-ARDS/non-COPD respiratory failure.

Study protocol After obtaining informed consent, enrolled patients were intubated and mechanically ventilated using the Mindray SV800 ventilator. An esophageal balloon catheter (SDY-1, Mindray, China) was inserted nasally to monitor respiratory mechanics [8]. The study did not interfere with the patients' ventilation modes or parameters. Chest wall compliance (Ccw) was measured at one timepoint during volume-controlled ventilation under sedation-induced apnea.

Thereafter, the ventilator automatically recorded waveforms (flow, pressure, volume, and esophageal pressure) along with the real-time calculated parameters N-Pmus and N-PTPmus.

- N-Pmus: The peak amplitude of Pmus(t) calculated using the novel algorithm during the patient's spontaneous inspiratory phase.
- N-PTPmus: The time integral of N-Pmus(t) during inspiration, reflecting the patient's total inspiratory muscle effort.

Esophageal pressure-derived metrics were used as the reference standard for validation:

- $Pmus_{eso}$: Calculated as the maximal difference between the esophageal pressure (Pes) and recoil pressure of the chest wall (Pcw, volume/Ccw) [8].

- $PTPmus_{eso}$: Obtained by integrating esophageal pressure-derived $Pmus_{eso}(t)$ over the inspiratory phase [8].

Statistical analysis

In the Bench study, each experimental scenario yielded a single averaged value, reducing the influence of repeated measurements. In the Clinical study, stable respiratory segments were selected based on predefined criteria for esophageal pressure and peak expiratory flow (see Figure E5). For each participant, 2 to 4 segments were identified, each comprising 20 consecutive breath cycles with consistent signal quality. These cycles were subsequently divided into 3 to 4 groups of 5 to 6 cycles each, and their averages were calculated to generate aggregated Pmus data. This approach effectively reduced intra-cycle variability [21] and minimized the influence of cardiac artifacts [22].

Data are presented as mean (standard deviation) or median [interquartile range], as appropriate.

Linear mixed-effects models were used to evaluate the association between N-Pmus, ASL5000-Pmus, and $Pmus_{eso}$, with patients treated as random effects [23]. Marginal R^2 and conditional R^2 were computed to quantify the variance in the dependent variable explained by the mixed models, excluding and including the variance attributed to random effects, respectively [24].

Bias and agreement were assessed using Bland–Altman analysis [25] for repeated measures. To account for repeated measures within patients, linear mixed-effects models were used to estimate within-patient limits of agreement and to compute the mean and between-patient standard deviation of the bias [26]. To address limited sample sizes, we used parametric bootstrap resampling to estimate 95% confidence intervals (CIs) [27].

Statistical analyses included the Wilcoxon tests. A p-value less than 0.05 was considered significant. Offline computation and aggregation of waveform data were performed using MATLAB (The MathWorks, Inc., Natick, MA, USA). Statistical analyses were conducted in RStudio (R Foundation for Statistical Computing, Vienna, Austria).

Results

The primary outcomes of this study include the correlation and agreement between N-Pmus and Pmus benchmarks (ASL5000-Pmus or $Pmus_{eso}$).

Bench study

A total of 270 scenarios were evaluated in the ASL5000 simulation experiment, simulating patients with different RC types, ventilation modes, Pmus amplitudes, and Pmus patterns. N-Pmus showed excellent correlation with ASL5000-Pmus, with a marginal R^2 of 0.993 and a conditional R^2 of 0.997 (Fig. 2(B)). The bias was −0.23 cmH_2O, and the limits of agreement ranged from −1.51 to 1.04 cmH_2O (Fig. 2(C)). Scenarios were further categorized into restrictive (across a range of compliances) and obstructive (across varying airway resistances) subgroups, with all demonstrating robust correlations (marginal $R^2 > 0.988$ and conditional $R^2 > 0.992$). Detailed clinical scenarios and simulation results are provided in Table E1 and Figure E4 in the Additional file.

Clinical study

Twenty-five patients initially met the inclusion criteria, but two were excluded due to absent of spontaneous breathing or missing of esophageal pressure data. The final analysis included 23 patients, with their clinical characteristics presented in Table 1. These patients contributed 1,380 single-cycle Pmus data pairs and 261 aggregated Pmus data pairs. The median number of aggregated data points per patient was 10 (IQR: 8–14), reflecting the number of distinct effort levels analyzed for each individual. As an example, representative tracings for Patient 16 are presented in Fig. 3(A), with the corresponding theoretical fit obtained using the N-Pmus algorithm shown in Fig. 3(B).

The analysis of aggregated Pmus data between N-Pmus and $Pmus_{eso}$ showed a marginal R^2 of 0.97 and a conditional R^2 of 0.971 (Fig. 4(B)). The bias was −0.2 cmH_2O, with limits of agreement ranging from −2.22 to 1.83 cmH_2O (Fig. 4(C)). In contrast, single-cycle data exhibited a correlation with a marginal R^2 of 0.884 and a conditional R^2 of 0.952 (Fig. 4(E)). The bias was −0.23 cmH_2O, with limits of agreement from −2.33 to 1.88 cmH_2O (Fig. 4(F)).

Furthermore, the correlation between N-PTPmus and $PTPmus_{eso}$ showed a marginal R^2 of 0.861 and a conditional R^2 of 0.907 (Fig. 5(B)). The bias was −0.18 $cmH_2O{\cdot}s$, with limits of agreement ranging from −2.45 to 2.08 $cmH_2O{\cdot}s$ (Fig. 5(C)).

Post-hoc subgroup analysis

Patients were stratified by disease type (COPD, ARDS, others). The ARDS subgroup demonstrated the strongest correlation between N-Pmus and $Pmus_{eso}$ (marginal R^2 = 0.955, conditional R^2 = 0.959; bias = −0.26 cmH_2O [95% CI: −0.75 to 0.35]), with limits of agreement (LOA) ranging from −2.87 to 2.35 cmH_2O. The COPD and other subgroups exhibited slightly lower correlations (COPD: marginal R^2 = 0.822, LOA = −1.85 to 1.47 cmH_2O; others: marginal R^2 = 0.876, LOA = −1.56 to 1.22 cmH_2O) (Table E2, Figure E6).

Analysis across ventilation modes (P-A/C, V-A/C, PSV, SIMV) revealed robust agreement, with V-A/C showing the highest correlation (marginal R^2 = 0.978, conditional R^2 = 0.982; bias = −0.06 cmH_2O [95% CI: −0.89 to 0.75]),

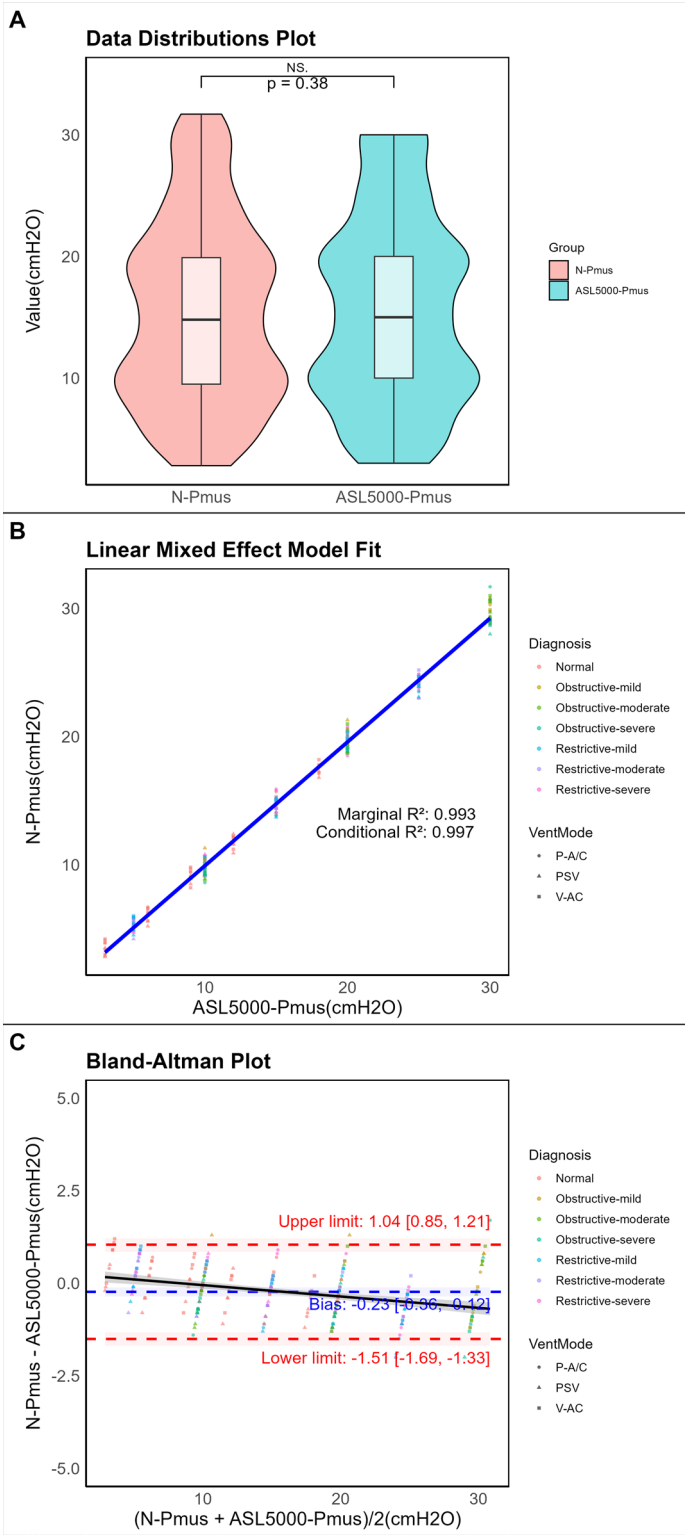

Fig. 2 Correlation and agreement analysis of Pmus parameter across ASL5000 test scenarios. (**A**) Violin plot depicting the Pmus measured by the ventilator (N-Pmus) and the Pmus settings from ASL5000 (ASL500-Pmus), with "NS" indicating no significant difference ($p > 0.05$). (**B**) Linear mixed-effects model fit plot showing the correlation between N-Pmus and ASL500-Pmus (marginal R^2=0.993, conditional R^2=0.997). (**C**) Corresponding Bland–Altman plot with a bias of –0.23 cmH_2O (95% CI: –0.36 to –0.12), L-LOA of – 1.51 cmH_2O (95% CI: –1.69 to – 1.33), and U-LOA of 1.04 cmH_2O (95% CI: 0.85 to 1.21). The linear regression of the bias is shown as the black line, illustrating the trend in the bias

Table 1 All patient's basic characteristics

No	Sex	Age (years)	BMI (kg/m^2)	Sub-group	Diagnosis	Depth† (cm)	OccRatio‡	Ccw (mL/cmH_2O)	Ventilation mode	TV (mL)	PEEP (cmH_2O)
1	M	43	28.6	ARDS	Necrotizing pancreatitis	57.5	1.01	107	PSV	416	12
2	M	51	25.1	Other	TAAA	60	1.09	175	V-A/C	438	10
3	M	64	22.5	Other	Coronary heart disease	65	0.87	206	P-A/C	456	10
4	M	74	24.5	ARDS	Severe acute pancreatitis	57.5	0.94	102	V-SIMV	420	12
5	F	23	18.7	Other	Autoimmune encephalitis	60	1.08	143	P-A/C	381	8
6	M	75	15.9	COPD	Emphysema	57.5	1.01	172	P-SIMV	474	8
7	M	53	26.0	ARDS	Type 1 RF	60	0.98	122	P-A/C	611	5
8	M	61	25.4	ARDS	Acute cerebral infarction	60	0.92	130	V-A/C	495	12
9	M	53	24.8	ARDS	Type 1 RF	60	0.93	360	PSV	608	6
10	M	72	22.9	ARDS	Pulmonary embolism	60	0.98	167	V-A/C	426	8
11	M	82	23.3	ARDS	Sepsis, Severe pneumonia	57.5	1.08	351	P-A/C	488	5
12	F	52	17.7	Other	Sepsis, Severe pneumonia	52.5	0.96	111	PSV	388	10
13	M	55	24.4	Other	Space-occupying lesion	60	1.08	333	P-A/C	754	5
14	M	87	21.3	COPD	Type 2 RF	65	0.98	165	P-A/C	472	8
15	F	87	28.9	COPD	Invasive aspergillosis	60	1.03	69	P-A/C	405	8
16	M	53	17.7	ARDS	Type 1 RF	57.5	1.07	76	PSV	391	8
17	M	56	25.6	COPD	End-stage renal disease	57.5	1.07	259	P-SIMV	401	8
18	F	79	27.5	COPD	AECOPD	60	0.99	84	PSV	358	8
19	F	58	20.2	Other	Traumatic brain injury	57.5	1.02	131	V-A/C	550	8
20	M	24	26.7	Other	Traumatic brain injury	55	1.03	222	P-A/C	503	10
21	F	74	18.7	COPD	AECOPD, Type 2 RF	51	1.08	112	PSV	351	5
22	M	75	23.0	COPD	AECOPD, Type 2 RF	57.5	0.96	91	V-A/C	397	8
23	M	61	26.0	COPD	Sepsis, AECOPD	57.5	1.2	141	P-A/C	520	8

Definition of abbreviations: BMI = body mass index; Ccw = compliance of the chest wall; TV = measured tidal volume; PEEP = positive end expiratory pressure; ARDS = acute respiratory distress syndrome; COPD = chronic obstructive pulmonary disease; TAAA = thoracoabdominal aortic aneurysm; RF = respiratory failure; AECOPD = acute exacerbation of chronic obstructive pulmonary disease;

† The transnasal esophageal balloon placement depth is measured from the nasal orifice to the catheter tip

‡ The ΔPes/ΔPaw ratio during the Baydur (occlusion) test with spontaneous breathing or the Positive Pressure Occlusion test without spontaneous breathing

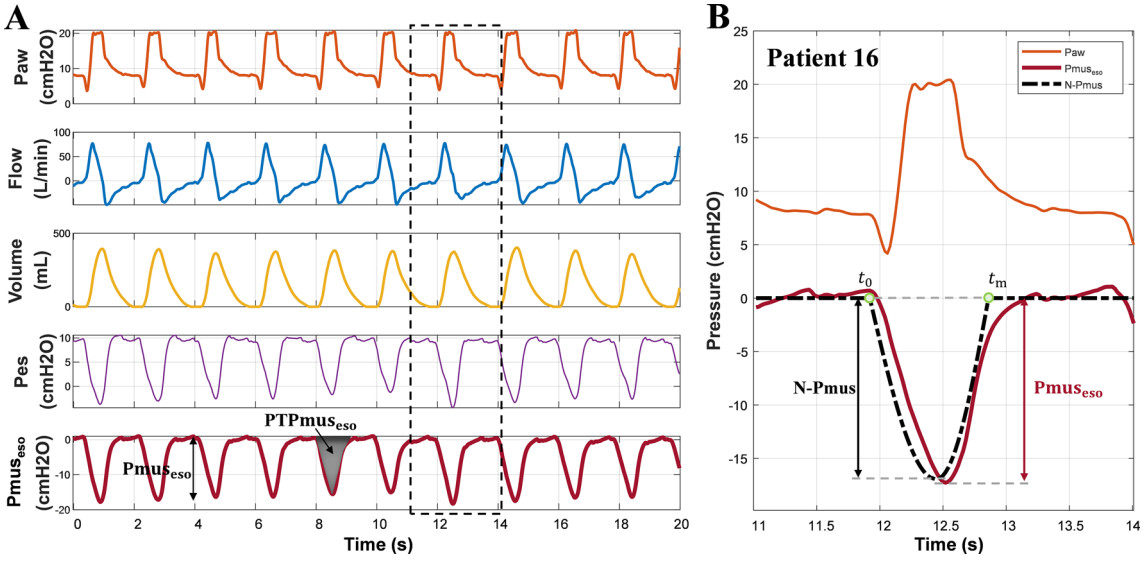

Fig. 3 Representative Tracings and Fitting Results of Pmus in Stable Breathing. (**A**) Representative tracings for Patient 16 during stable breathing, obtained through ventilator measurements or calculations, including airway pressure (Paw), flow, volume, and esophageal pressure (Pes) signals recorded by the ventilator. Pmus, estimated as the difference between Chest wall elastic recoil pressure (Pcw) and Pes (baseline Pmus defined as 0 cm H_2O), was quantified by the peak inspiratory muscle pressure ($Pmus_{eso}$) and the pressure–time product of Pmus per breath ($PTPmus_{eso}$). (**B**) Typical fitting results using the non-invasive Pmus algorithm. The algorithm calculates the onset ($\mathbf{t_0}$) and offset ($\mathbf{t_m}$) of respiratory muscle activity. The red solid line represents the $Pmus_{eso}$ waveform, while the black solid line represents the N-Pmus waveform, with N-Pmus quantified identically to $Pmus_{eso}$ for data analysis

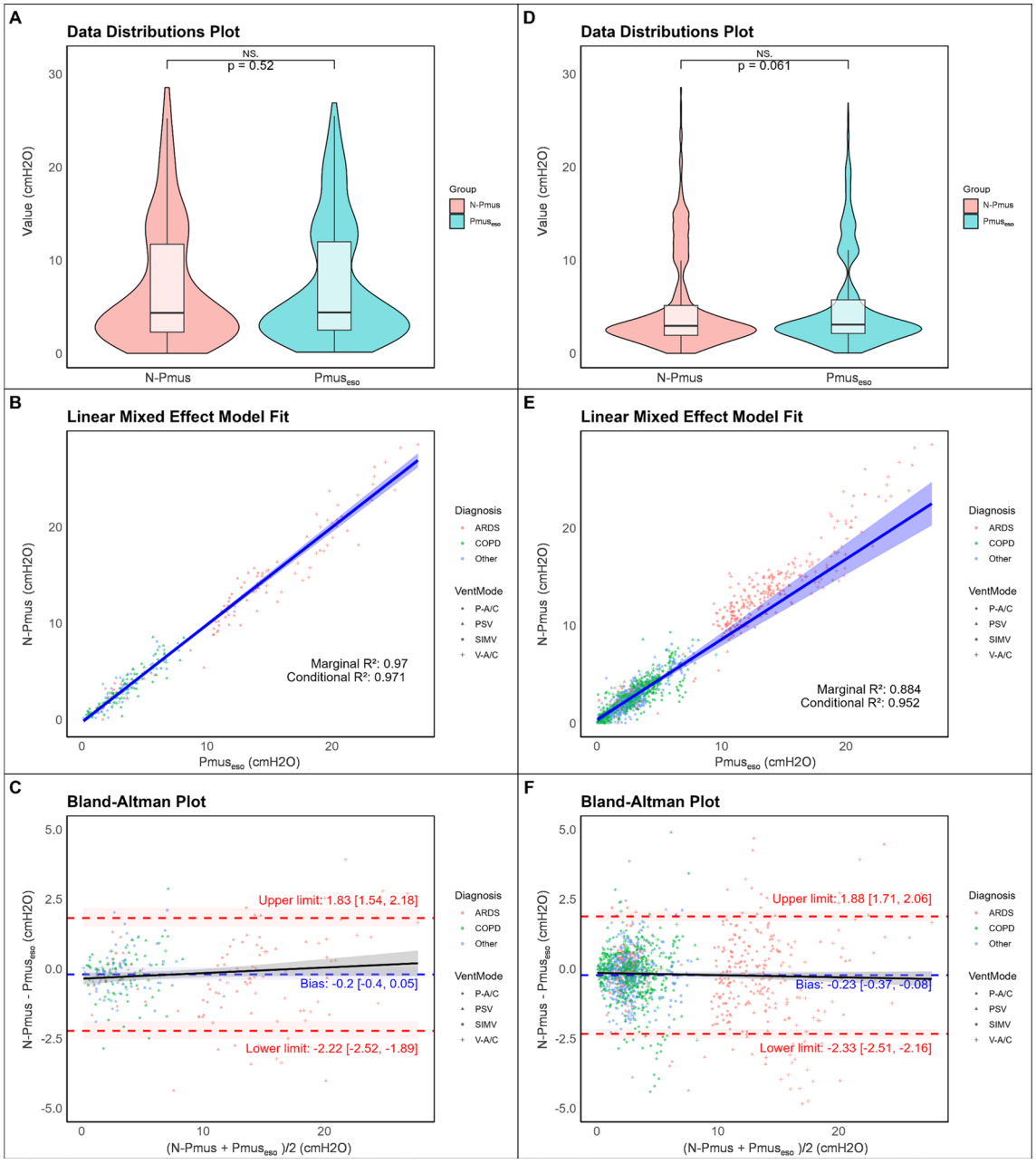

Fig. 4 Correlation and agreement analysis between N-Pmus and $Pmus_{eso}$ for patient data from the clinical trial. (**A**), (**B**), and (**C**) display the analysis results for aggregated Pmus data across varying levels of inspiratory effort, while (**D**), (**E**), and (**F**) show the analysis results for single-cycle Pmus data. (**A**) and (**D**) are violin plots depicting the Pmus measured by the ventilator (N-Pmus) and the gold-standard Pmus calculated using esophageal pressure ($Pmus_{eso}$), with "NS" indicating no significant difference ($p > 0.05$). (**B**) and (**E**) show linear mixed-effects model fit plots demonstrating the correlation between N-Pmus and $Pmus_{eso}$, where (**B**) has marginal R^2=0.97 and conditional R^2=0.971, and (**E**) has marginal R^2=0.884 and conditional R^2=0.952. (**C**) and (**F**) are the corresponding Bland–Altman plots, where (**C**) has a bias of −0.2 cmH_2O (95% CI: −0.4 to −0.05), L-LOA of − 2.22 cmH_2O (95% CI: −2.52 to − 1.89), and U-LOA of 1.83 cmH_2O (95% CI: 1.54 to 2.18), while (F) has a bias of −0.23 cmH_2O (95% CI: −0.37 to − 0.08), L-LOA of − 2.33 cmH_2O (95% CI: −2.51 to − 2.16), and U-LOA of 1.88 cmH_2O (95% CI: 1.71 to 2.06). The linear regression of the bias is shown as the black line, illustrating the trend in the bias

and LOA ranging from − 2.88 to 2.76 cmH_2O. P-A/C, PSV, and SIMV modes demonstrated narrower LOA ranges (P-A/C: −2.04 to 1.18 cmH_2O; PSV: −2.46 to 2.17 cmH_2O; SIMV: −1.48 to 1.45 cmH_2O) (Table E3, Figure E7).

Stratification by $Pmus_{eso}$ magnitude (low: <4 cmH_2O; normal: 4–10 cmH_2O; high: >10 cmH_2O) revealed stronger correlations in the high-effort group (marginal R^2 = 0.895, conditional R^2 = 0.916; bias = − 0.12 cmH_2O [95% CI: −1.1 to 0.59]), with LOA spanning from − 3.04 to 2.79 cmH_2O. The low- and normal-effort groups

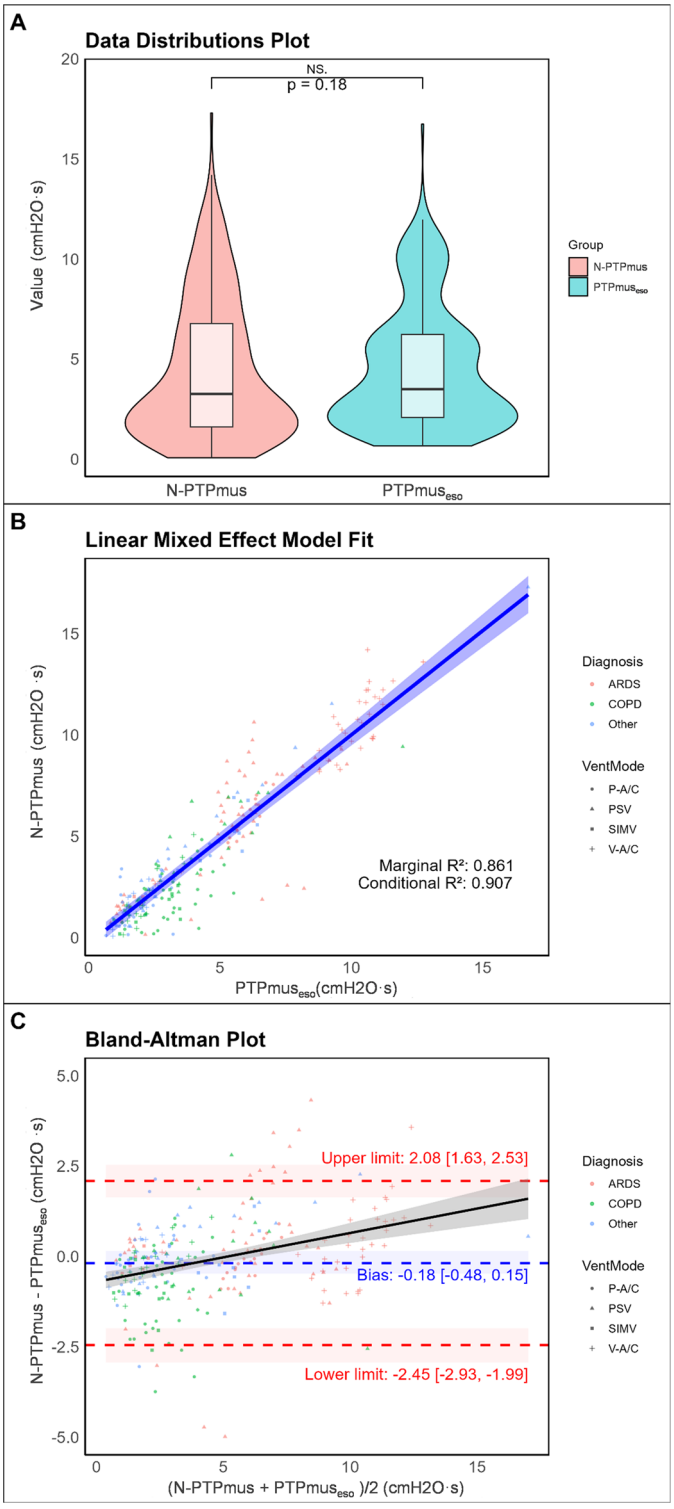

Fig. 5 Correlation and agreement analysis between N-PTPmus and $PTPmus_{eso}$ for patient data from the clinical trial. (**A**) Violin plot depicting the PTPmus values measured by the ventilator (N-PTPmus) and the usual monitoring PTPmus values calculated using esophageal pressure ($PTPmus_{eso}$), with "NS" indicating no significant difference ($p > 0.05$). (**B**) Linear mixed-effects model fit plot showing the correlation between N-PTPmus and $PTPmus_{eso}$ (marginal R^2=0.861, conditional R^2=0.907). (**C**) Corresponding Bland–Altman plot with a bias of −0.18 $cmH_2O{\cdot}s$ (95% CI: −0.48 to − 0.15), L-LOA of − 2.45 $cmH_2O{\cdot}s$ (95% CI: −2.93 to − 1.99), and U-LOA of 2.08 $cmH_2O{\cdot}s$ (95% CI: 1.63 to 2.53). The linear regression of the bias is shown as the black line, illustrating the trend in the bias

exhibited reduced agreement (low: marginal R^2 = 0.611, LOA = – 1.46 to 0.97 cmH_2O; normal: marginal R^2 = 0.628, LOA = – 2.38 to 1.65 cmH_2O) (Table E4, Figure E8).

Discussion

In this investigation, we introduced and validated N-Pmus, an innovative non-invasive approach for continuous, real-time monitoring of respiratory effort at the bedside in mechanically ventilated patients. The essence of the N-Pmus algorithm lies in integrating a functional model with physiological constraints into the equation governing respiratory motion, solving it iteratively via the least squares method. A bench study conducted in a simulated setting demonstrated a perfect correlation of 0.99 between N-Pmus and ASL5000-Pmus, with narrow 95% limits of agreement of [–1.51, 1.04] cmH_2O. Additionally, a subsequent clinical validation study showcased a high correlation of 0.97 between N-Pmus and $Pmus_{eso}$, with tight 95% limits of agreement of [–2.22, 1.83] cmH_2O. Subsequent subgroup analyses post hoc unveiled a robust correlation and excellent agreement across diverse disease categories, ventilation modalities, and degrees of respiratory effort.

Feasible and reliable monitoring of respiratory effort in mechanically ventilated patients is paramount to mitigate potential lung and diaphragm injuries. Currently, the accuracy of both direct monitoring techniques (Pes and Pdi) and indirect methods (P0.1, PMI, and Pocc) can be susceptible to various factors including procedural standards, the state of illness, and the respiratory status of patients [28] impeding seamless real-time monitoring. Notably, Albani et al. [29, 30] proposed a noninvasive real-time monitoring technique for inspiratory effort by analyzing the concavity of the inspiratory flow waveform in pressure support ventilation (PSV). However, this method is restricted to PSV and lacks automated calculation capabilities. Pmus, recognized as a key indicator of respiratory effort, has been a focal point of research for achieving noninvasive real-time monitoring.

In reviewing decades of research, methodologies for real-time Pmus calculation using respiratory mechanics equations can be categorized into two main approaches. The first approach entails solving for respiratory system resistance and compliance before back-calculating the Pmus waveform [16, 31–36]. The second approach involves simultaneously determining Pmus, resistance, and compliance while incorporating constraints into the motion Eqs. [37–39]. Previous studies often underestimate Pmus because active respiratory muscle effort distorts airway pressure and flow profiles, leading to inaccuracies when such activity is not fully accounted for [37–39]. In contrast, our algorithm enhances Pmus estimation by employing global constrained least-squares fitting, a cubic function template to model active expiration, and advanced waveform feature recognition using both inspiratory and expiratory data. These advancements significantly improved the accuracy of Pmus peak estimation and morphology characterization, as detailed in the Additional file (see Figure E2 and Figure E3). Validation of this approach is conducted through simulation studies and clinical trials, offering promising prospects for enhanced respiratory effort monitoring in mechanically ventilated patients.

The simulation experiment validated scenarios encompassing prevalent disease types, including restrictive and obstructive lung diseases, as well as typical ventilator mode settings, such as V-A/C, P-A/C, PSV, and SIMV, commonly seen in clinical practice. The high correlation, reaching up to 0.99, can be ascribed to the meticulous mathematical model of the Pmus waveform generated by the ASL5000 and the precise fitting effect of the theoretical model. The 95% limits of agreement were found to be [–1.51, 1.04] cmH_2O. Furthermore, Silva et al. [39] simulated 49 scenarios, revealing that deviations from the absolute Pmus amplitude predominantly clustered within the quartiles (0.4 to 1.3 cmH_2O). Our simulation experiments confirmed similar outcomes across a wider range of use case scenarios, including those with elevated resistance and decreased compliance. However, it should be noted that the observed correlation may be influenced by the method of effort generation used by the ASL5000, which warrants further investigation to assess its generalizability.

In our clinical trial with 23 patients, the correlation between N-Pmus and $Pmus_{eso}$ was 0.97, with 95% limits of agreement from – 2.22 to 1.83 cmH_2O. This demonstrates significantly improved accuracy and reproducibility compared to previous studies, particularly that of Kondili et al. [34], who estimated Pmus by applying historical measurements of resistance and compliance to the equation of motion in 11 patients (correlation of 0.83; 95% limits of agreement from – 7.23 to 5.41 cmH_2O), and Natalini et al. [35], who studied 18 patients (correlation of 0.58; 95% limits of agreement from – 12 to 12 cmH_2O). Similarly, the correlation between N-PTPmus and $PTPmus_{eso}$ was 0.86, with 95% limits of agreement from – 2.45 to 2.08 $cmH_2O{\cdot}s$, surpassing the findings of Kondili et al. [34] (correlation of 0.77, 95% limits of agreement between – 3.01 and 1.99 $cmH_2O{\cdot}s$), and Natalini et al. [35] (correlation of 0.52, 95% limits of agreement between – 8.35 and 7.74 $cmH_2O{\cdot}s$).

In a post-hoc subgroup analysis, the ARDS subgroup showed the highest correlation between N-Pmus and $Pmus_{eso}$ (marginal R^2 = 0.955) but exhibited a wide limit of agreement (LOA: –2.87 to 2.35 cmH_2O). In contrast, the COPD and other disease subgroups demonstrated lower correlations (COPD: marginal R^2 = 0.822; others: marginal R^2 = 0.876) with narrower LOA. Stratification

by respiratory effort revealed that the high-effort group, similar to the ARDS subgroup, had the highest correlation with a wider LOA, whereas the normal and low-effort groups had lower correlations and narrower LOA. These differences are primarily attributable to the influence of respiratory effort magnitude on measurement precision: in high-effort states (commonly observed in ARDS), larger Pmus values reduce the relative impact of small absolute errors—enhancing correlation—but also amplify absolute differences. In practice, the relative error remains small, yet this leads to a wider LOA. Conversely, in low-effort states (as seen in other subgroups), smaller Pmus values exaggerate the relative effect of minimal errors, leading to lower correlations but narrower LOA. Therefore, further investigations are imperative to validate the observations within this subgroup.

Strengths and limitations

This study systematically presents the derivation of the N-Pmus algorithm along with the results from laboratory simulations and clinical validation. The simulation scenarios strived to cover a broad spectrum of patient profiles, Pmus configurations, and a wide array of amplitudes, while the clinical trials aimed to confirm the efficacy across diverse patient phenotypes. Nonetheless, our study does have certain limitations. Firstly, while esophageal pressure serves as the most accurate approximation of pleural pressure, it may not accurately represent the actual intrathoracic pressure under various pathological conditions. Although chest wall compliance typically remains relatively constant, patients subjected to differing circumstances, such as controlled versus spontaneous ventilation, might exhibit slightly varying effects on this compliance. Thus, the aforementioned limitations regarding the discrepancy between $Pmus_{eso}$ in the control group and the true Pmus necessitate further refinement. Secondly, the study is constrained by its brief duration, diminutive sample size, and confinement to a single center. Finally, it omitted the inclusion of healthy subjects or individuals with specific conditions like abdominal hypertension, and it did not assess transdiaphragmatic pressure (Pdi). Subsequent validation endeavors should incorporate long term, more extensive, multicenter research initiatives.

Conclusions

This study introduces an innovative, bedside, non-invasive, real-time approach to quantitatively evaluate respiratory effort. Our investigation illustrated that N-Pmus showcases a robust correlation and agreement with the established Pmus benchmarks (ASL5000-Pmus or $Pmus_{eso}$), surpassing conventional metrics for assessing respiratory effort. Further research is essential to validate this technique and explore its clinical applications. In the future, N-Pmus will enable precise monitoring and guide parameter adjustments in mechanical ventilation, potentially supporting lung- and diaphragm-protective ventilation.

Abbreviations

Pmus	Respiratory muscle pressure
Pes	Esophageal pressure
Pcw	Chest wall elastic recoil pressure
Ccw	Compliance of the chest wall
N-Pmus	Real-time Pmus amplitude monitored by the ventilator
$Pmus_{eso}$	The usual monitoring for Pmus amplitude, calculated from Pes and Pcw
ASL5000-Pmus	Pmus settings from ASL5000
N-PTPmus	Pressure–time-product of Pmus measured by the ventilator in a single breath
$PTPmus_{eso}$	The usual monitoring pressure–time-product of Pmus, calculated using esophageal pressure in a single breath
P-A/C	Pressure-assist/control ventilation
PSV	Pressure support ventilation

Supplementary Information

The online version contains supplementary material available at https://doi.org/10.1186/s13054-025-05514-4.

Supplementary Material 1

Acknowledgements

Not applicable.

Author contributions

Study concept and design: YL, MD, HS, ZH, YZ, JL and BW. Acquisition of data: YL, ZN, ZW and XJ. Analysis and interpretation of data: YL, MD, HS, ZH, YZ, JL and BW. Drafting of the manuscript: MD, HS and YZ. Critical revision and important intellectual contribution: YL, MD, HS, ZH, YZ, JL and BW. Statistical analysis: HS, ZH and JL. Administrative support: XZ, JL, BW and YK. Study supervision: YZ, JL, BW and YK.

Funding

This study received funding from Mindray (China).

Data availability

No datasets were generated or analysed during the current study.

Declarations

Ethics approval and consent to participate

This study was performed in line with the principles of the Declaration of Helsinki. Approval was granted by the Ethics Committee of West China Hospital, Sichuan University (Ethics Approval No. 2023 Approval (105)). Written informed consent was obtained from the legal primary decision-maker, who was the spouse of the patient, or the parent of the child in cases in which there was no spouse. The trial was registered at chictr.org.cn (ChiCTR2300076940).

Consent for publication

Not applicable.

Competing interests

The authors declare no competing interests.

Received: 22 January 2025 / Accepted: 18 June 2025
Published online: 03 July 2025

References

1. Slutsky AS, Ranieri VM. Ventilator-Induced lung injury. N Engl J Med. 2013;369(22):2126–36.
2. Amato MB, Meade MO, Slutsky AS, Brochard L, Costa EL, Schoenfeld DA, Stewart TE, Briel M, Talmor D, Mercat A, et al. Driving pressure and survival in the acute respiratory distress syndrome. N Engl J Med. 2015;372(8):747–55.
3. Urner M, Juni P, Hansen B, Wettstein MS, Ferguson ND, Fan E. Time-varying intensity of mechanical ventilation and mortality in patients with acute respiratory failure: a registry-based, prospective cohort study. Lancet Respir Med. 2020;8(9):905–13.
4. Yoshida T, Grieco DL, Brochard L, Fujino Y. Patient self-inflicted lung injury and positive end-expiratory pressure for safe spontaneous breathing. Curr Opin Crit Care. 2020;26(1):59–65.
5. Demoule A, Molinari N, Jung B, Prodanovic H, Chanques G, Matecki S, Mayaux J, Similowski T, Jaber S. Patterns of diaphragm function in critically ill patients receiving prolonged mechanical ventilation: a prospective longitudinal study. Ann Intensive Care. 2016;6(1):75.
6. Goligher EC, Dres M, Fan E, Rubenfeld GD, Scales DC, Herridge MS, Vorona S, Sklar MC, Rittayamai N, Lanys A, et al. Mechanical Ventilation-induced diaphragm atrophy strongly impacts clinical outcomes. Am J Respir Crit Care Med. 2018;197(2):204–13.
7. Cherniack RM, Farhi LE, Armstrong BW, Proctor DF. A comparison of esophageal and intrapleural pressure in man. J Appl Physiol. 1955;8(2):203–11.
8. Akoumianaki E, Maggiore SM, Valenza F, Bellani G, Jubran A, Loring SH, Pelosi P, Talmor D, Grasso S, Chiumello D, et al. The application of esophageal pressure measurement in patients with respiratory failure. Am J Respir Crit Care Med. 2014;189(5):520–31.
9. Foti G, Cereda M, Banfi G, Pelosi P, Fumagalli R, Pesenti A. End-inspiratory airway occlusion: a method to assess the pressure developed by inspiratory muscles in patients with acute lung injury undergoing pressure support. Am J Respir Crit Care Med. 1997;156(4 Pt 1):1210–6.
10. Bertoni M, Telias I, Urner M, Long M, Del Sorbo L, Fan E, Sinderby C, Beck J, Liu L, Qiu H, et al. A novel non-invasive method to detect excessively high respiratory effort and dynamic transpulmonary driving pressure during mechanical ventilation. Crit Care (London England). 2019;23(1):346.
11. Bellani G, Mauri T, Coppadoro A, Grasselli G, Patroniti N, Spadaro S, Sala V, Foti G, Pesenti A. Estimation of patient's inspiratory effort from the electrical activity of the diaphragm. Crit Care Med. 2013;41(6):1483–91.
12. Jansen D, Jonkman AH, Roesthuis L, Gadgil S, van der Hoeven JG, Scheffer GJ, Girbes A, Doorduin J, Sinderby CS, Heunks LMA. Estimation of the diaphragm neuromuscular efficiency index in mechanically ventilated critically ill patients. Crit Care. 2018;22(1):238.
13. Goligher EC, Laghi F, Detsky ME, Farias P, Murray A, Brace D, Brochard LJ, Bolz SS, Rubenfeld GD, Kavanagh BP, et al. Measuring diaphragm thickness with ultrasound in mechanically ventilated patients: feasibility, reproducibility and validity. Intensive Care Med. 2015;41(4):642–9.
14. Bertoni M, Spadaro S, Goligher EC. Monitoring patient respiratory effort during mechanical ventilation: lung and Diaphragm-Protective ventilation. Crit Care. 2020;24(1):106.
15. Jonkman AH, de Vries HJ, Heunks LMA. Physiology of the respiratory drive in ICU patients: implications for diagnosis and treatment. Crit Care. 2020;24(1):104.
16. Iotti GA, Braschi A, Brunner JX, Smits T, Olivei M, Palo A, Veronesi R. Respiratory mechanics by least squares fitting in mechanically ventilated patients: applications during paralysis and during pressure support ventilation. Intensive Care Med. 1995;21(5):406–13.
17. Arnal JM, Garnero A, Saoli M, Chatburn RL. Parameters for simulation of adult subjects during mechanical ventilation. Respir Care. 2018;63(2):158–68.
18. Daoud EG, Katigbak R, Ottochian M. Accuracy of the ventilator automated displayed respiratory mechanics in passive and active breathing conditions: A bench study. Respir Care. 2019;64(12):1555–60.
19. Force ADT, Ranieri VM, Rubenfeld GD, Thompson BT, Ferguson ND, Caldwell E, Fan E, Camporota L, Slutsky AS. Acute respiratory distress syndrome: the Berlin definition. JAMA. 2012;307(23):2526–33.
20. Disease GICOL. Global Strategy for the Diagnosis, Management, and Prevention of Chronic Obstructive Pulmonary Disease (2023 Report). In.; 2023.
21. Bellani G, Bronco A, Arrigoni Marocco S, Pozzi M, Sala V, Eronia N, Villa G, Foti G, Tagliabue G, Eger M, et al. Measurement of diaphragmatic electrical activity by surface electromyography in intubated subjects and its relationship with inspiratory effort. Respir Care. 2018;63(11):1341–9.
22. Qin Y, Huang Z, Zhou X, Gui S, Xiong L, Liu L, Liu J. A novel adaptive filter with a heart-rate-based reference signal for esophageal pressure signal denoising. J Clin Monit Comput 2024 38(5):1125–1134. https://doi.org/10.1007/s10877-023-01116-z.
23. Shan G, Zhang H, Jiang T. Correlation Coefficients for a Study with Repeated Measures. *Comput Math Methods Med* 2020, 2020:7398324.
24. Nakagawa S, Schielzeth H, O'Hara RB. A general and simple method for obtaining R2 from generalized linear mixed-effects models. Methods Ecol Evol. 2012;4(2):133–42.
25. Martin Bland J, Altman D. Statistical methods for assessing agreement between two methods of clinical measurement. Lancet. 1986;327(8476):307–10.
26. Myles PS, Cui J. Using the Bland-Altman method to measure agreement with repeated measures. Br J Anaesth. 2007;99(3):309–11.
27. Parker RA, Weir CJ, Rubio N, Rabinovich R, Pinnock H, Hanley J, McCloughan L, Drost EM, Mantoani LC, MacNee W, et al. Application of mixed effects limits of agreement in the presence of multiple sources of variability: exemplar from the comparison of several devices to measure respiratory rate in COPD patients. PLoS ONE. 2016;11(12):e0168321.
28. Spinelli E, Mauri T, Beitler JR, Pesenti A, Brodie D. Respiratory drive in the acute respiratory distress syndrome: pathophysiology, monitoring, and therapeutic interventions. Intensive Care Med. 2020;46(4):606–18.
29. Albani F, Fusina F, Ciabatti G, Pisani L, Lippolis V, Franceschetti ME, Giovannini A, di Mussi R, Murgolo F, Rosano A, et al. Flow index accurately identifies breaths with low or high inspiratory effort during pressure support ventilation. Crit Care. 2021;25(1):427.
30. Albani F, Pisani L, Ciabatti G, Fusina F, Buizza B, Granato A, Lippolis V, Aniballi E, Murgolo F, Rosano A, et al. Flow index: a novel, non-invasive, continuous, quantitative method to evaluate patient inspiratory effort during pressure support ventilation. Crit Care. 2021;25(1):196.
31. Gillard C, Flemale A, Dierckx JP, Themelin G. Measurement of effective elastance of the total respiratory system in ventilated patients by a computed method. Comparison with the static method. Intensive Care Med. 1990;16(3):189–95.
32. Lucangelo U, Bernabe F, Blanch L. Respiratory mechanics derived from signals in the ventilator circuit. Respir Care. 2005;50(1):55–65. discussion 65–57.
33. Younes M, Brochard L, Grasso S, Kun J, Mancebo J, Ranieri M, Richard J-C, Younes H. A method for monitoring and improving patient: ventilator interaction. Intensive Care Med. 2007;33(8):1337–46.
34. Kondili E, Alexopoulou C, Xirouchaki N, Vaporidi K, Georgopoulos D. Estimation of inspiratory muscle pressure in critically ill patients. Intensive Care Med. 2010;36(4):648–55.
35. Natalini G, Buizza B, Granato A, Aniballi E, Pisani L, Ciabatti G, Lippolis V, Rosano A, Latronico N, Grasso S, et al. Non-invasive assessment of respiratory muscle activity during pressure support ventilation: accuracy of end-inspiration occlusion and least square fitting methods. J Clin Monit Comput. 2021;35(4):913–21.
36. Gutierrez G. A non-invasive method to monitor respiratory muscle effort during mechanical ventilation. J Clin Monit Comp 2024 38(3):701–714. https://doi.org/10.1007/s10877-024-01164-z.
37. Vicario F, Albanese A, Wang D, Karamolegkos N, Chbat NW. Ieee: Constrained Optimization for Noninvasive Estimation of Work of Breathing. In: *2015 37TH ANNUAL INTERNATIONAL CONFERENCE OF THE IEEE ENGINEERING IN MEDICINE AND BIOLOGY SOCIETY (EMBC).* 2015: 5327–5330.
38. Vicario F, Albanese A, Karamolegkos N, Wang D, Seiver A, Chbat NW. Non-invasive Estimation of respiratory mechanics in spontaneously breathing ventilated patients: A constrained optimization approach. IEEE Trans Biomed Eng. 2016;63(4):775–87.
39. Silva DO, de Souza PN, de Araujo Sousa ML, Morais CCA, Ferreira JC, Holanda MA, Yamaguti WP, Junior LP, Costa ELV. Impact on the ability of healthcare professionals to correctly identify patient-ventilator asynchronies of the simultaneous visualization of estimated muscle pressure curves on the ventilator display: a randomized study (Pmus study). Crit Care 2023, 27(1):128. https://doi.org/10.1186/s13054-023-04414-9.

Publisher's note